CYP76AH1 catalyzes turnover of miltiradiene in tanshinones biosynthesis and enables heterologous production of ferruginol in yeasts

Juan Guo[a,1], Yongjin J. Zhou[b,1], Matthew L. Hillwig[c], Ye Shen[a], Lei Yang[d], Yajun Wang[a], Xianan Zhang[a], Wujun Liu[b], Reuben J. Peters[c,2], Xiaoya Chen[d], Zongbao K. Zhao[b,2], and Luqi Huang[a,2]

[a]National Resource Center for Chinese Materia Medica, China Academy of Chinese Medical Sciences, Beijing 100700, People's Republic of China; [b]Division of Biotechnology, Dalian Institute of Chemical Physics, Chinese Academy of Sciences, Dalian 116023, People's Republic of China; [c]Department of Biochemistry, Biophysics, and Molecular Biology, Iowa State University, Ames, IA 50011; and [d]National Key Laboratory of Plant Molecular Genetics, Institute of Plant Physiology and Ecology, and Plant Science Research Center of Shanghai Chenshan Botanical Garden, Shanghai Institutes for Biological Sciences, Chinese Academy of Sciences, Shanghai 200032, People's Republic of China

Edited by Joseph P. Noel, Howard Hughes Medical Institute and The Salk Institute for Biological Studies, La Jolla, CA, and accepted by the Editorial Board May 22, 2013 (received for review October 16, 2012)

Cytochrome P450 enzymes (CYPs) play major roles in generating highly functionalized terpenoids, but identifying the exact biotransformation step(s) catalyzed by plant CYP in terpenoid biosynthesis is extremely challenging. Tanshinones are abietane-type norditerpenoid naphthoquinones that are the main lipophilic bioactive components of the Chinese medicinal herb danshen (*Salvia miltiorrhiza*). Whereas the diterpene synthases responsible for the conversion of (*E,E,E*)-geranylgeranyl diphosphate into the abietane miltiradiene, a potential precursor to tanshinones, have been recently described, molecular characterization of further transformation of miltiradiene remains unavailable. Here we report stable-isotope labeling results that demonstrate the intermediacy of miltiradiene in tanshinone biosynthesis. We further use a next-generation sequencing approach to identify six candidate CYP genes being coregulated with the diterpene synthase genes in both the rhizome and danshen hairy roots, and demonstrate that one of these, CYP76AH1, catalyzes a unique four-electron oxidation cascade on miltiradiene to produce ferruginol both in vitro and in vivo. We then build upon the previous establishment of miltiradiene production in *Saccharomyces cerevisiae*, with incorporation of CYP76AH1 and phyto-CYP reductase genes leading to heterologous production of ferruginol at 10.5 mg/L. As ferruginol has been found in many plants including danshen, the results and the approaches that were described here provide a solid foundation to further elucidate the biosynthesis of tanshinones and related diterpenoids. Moreover, these results should facilitate the construction of microbial cell factories for the production of phytoterpenoids.

phytoterpenoids biosynthesis | gene discovery | synthetic pathway | metabolic engineering

Terpenoids represent a diverse class of secondary metabolites attracting commercial interest due to their use as drugs, fragrances, and alternative fuels. In plants, terpenoids are synthesized from two C_5 precursors, isopentenyl diphosphate (IPP) and dimethylallyl diphosphate (DMAPP), which are derived via the 1-deoxyxylulose-5-phosphate pathway or the mevalonate pathway. Prenyltransferases then combine DMAPP and IPP to form other building blocks, (*E*)-geranyl pyrophosphate (GPP; C_{10}), (*E,E*)-farnesyl pyrophosphate (FPP; C_{15}), and (*E,E,E*)-geranylgeranyl pyrophosphate (GGPP; C_{20}). These acyclic precursors are transformed by terpene synthases/cyclases, followed by tailoring enzymes to generate compounds with tremendous structure diversities. Thus, over 50,000 terpenoid compounds have been identified. The most important tailoring process in terpenoid biosynthesis is oxidation/oxygenation, which is largely catalyzed by cytochrome P450 (CYP) enzymes (1). However, functionally characterizing the role of plant CYP in particular biotransformation step(s) in terpenoid biosynthesis is extremely challenging, because these CYPs normally have high substrate specificity, share low sequence homology (2), and the encoding genes generally are not physically clustered together with genes responsible for the upstream enzymatic reactions as found in microbial genomes (3). For example, despite tremendous efforts during the past two decades to delineate the biosynthetic pathway for the most important diterpenoid, taxol, there are still unresolved steps likely involving transformations catalyzed by CYP (4). Nonetheless, research continues, and has even intensified, because understanding the molecular basis of terpenoid biosynthesis holds great promise to engineer the native-producing organisms, as well as surrogate microbes, to produce the desired molecules in sufficient quantities for commercial purposes.

Our recent efforts have been focused on the biosynthesis of a group of abietane-type norditerpenoids, tanshinones (Fig. 1), the major lipophilic bioactive components of the rhizome of the Chinese medicinal herb, *Salvia miltiorrhiza* Bunge (Lamiaceae), known as tanshen or danshen (5). Danshen has been prominently mentioned in discussions of how traditional Chinese medicine might be coupled to a more modern approach (6). More importantly, tanshinones have been shown to exhibit a variety of biological activities, which includes antibiotic, anti-inflammatory, and antioxidant effects, as well as activity against various aspects of heart disease. Indeed, danshen preparations are in phase II clinical trials against cardiovascular disease (7). Although the production of tanshinones is inducible in *S. miltiorrhiza* hairy roots (8), the current supply is dependent on field-grown plants, which are subject to variable yields, and genetic modification offers potentially increased yields in either system. However, this requires some understanding of the underlying biosynthetic pathway. Our initial investigations were carried out using a functional genomics approach based on a cDNA microarray using ~4,400 expressed sequence tags (ESTs), generated with traditional sequencing technology (9). This led to functional identification of two sequentially acting diterpene cyclases, as required for the formation of labdane-related diterpenoids such as the tanshinones (10, 11): specifically, a class II diterpene cyclase, which produces copalyl diphosphate from GGPP, termed CPP synthase (SmCPS), and a subsequently

Author contributions: J.G., Y.J.Z., R.J.P., X.C., Z.K.Z., and L.H. designed research; J.G., Y.J.Z., M.L.H., Y.S., Y.W., X.Z., and W.L. performed research; X.C. contributed new reagents/analytic tools; J.G., Y.J.Z., M.L.H., Y.S., L.Y., R.J.P., Z.K.Z., and L.H. analyzed data; and J.G., Y.J.Z., R.J.P., Z.K.Z., and L.H. wrote the paper.

The authors declare no conflict of interest.

This article is a PNAS Direct Submission. J.P.N. is a guest editor invited by the Editorial Board.

Data deposition: The sequences reported in this paper have been deposited in the GenBank database (accession nos. SRX224100, JX422213–JX422218, and CBX24555).

[1]J.G. and Y.J.Z. contributed equally to this work.

[2]To whom correspondence may be addressed. E-mail: zhaozb@dicp.ac.cn, rjpeters@iastate.edu, or huangluqi@263.net.

This article contains supporting information online at www.pnas.org/lookup/suppl/doi:10.1073/pnas.1218061110/-/DCSupplemental.

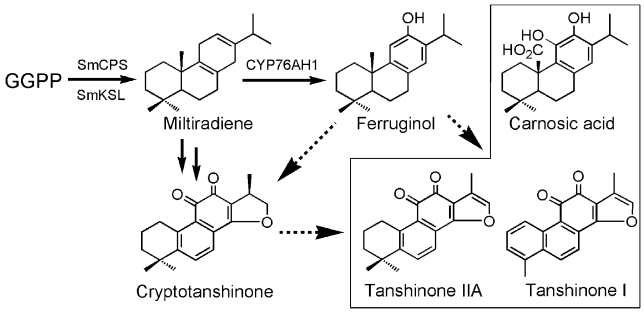

Fig. 1. Partial pathways for tanshinones biosynthesis and structures for some representative tanshinones. Solid arrows indicate the established relationships, and dashed arrows indicate hypothetical relationships.

acting class I diterpene cyclase, termed *ent*-kaurene synthase-like (SmKSL), which produces the abietane miltiradiene (11).

Miltiradiene contains a cyclohexa-1,4-diene moiety that imposes a planar configuration on the distal ring, which is suggestively poised for aromatization, as required for the production of tanshinones. Thus, miltiradiene is a potential intermediate in tanshinone biosynthesis, albeit requiring extensive tailoring steps involving oxidation/oxygenation as well as carbon–carbon bond scission (Fig. 1). However, information remains unavailable for structural tailoring miltiradiene and downstream steps of tanshinone biosynthesis at the molecular level. Here we describe results that demonstrate the intermediacy of miltiradiene, at least for late intermediates in the tanshinone biosynthetic pathway, as well as the use of a next-generation sequencing approach to functionally identify a CYP, miltiradiene oxidase CYP76AH1, able to convert miltiradiene to ferruginol. We show that synthetic pathways incorporating CYP76AH1 upon previously engineered *Saccharomyces cerevisiae* (12) enable the production of this elaborated phytoterpenoid up to 10.5 mg/L, providing a platform for further investigation of derived natural products such as the tanshinones.

Results

Intermediacy of Miltiradiene in Tanshinone Biosynthesis. Whereas the planar conformation of the distal ring in miltiradiene is suggestive, a role for miltiradiene in tanshinone biosynthesis remained hypothetical. This was investigated by stable-isotope labeling. To generate labeled miltiradiene we used a previously developed *Escherichia coli*-based metabolic engineering system that enables coexpression of SmCPS and SmKSL with a GGPP synthase (13), along with up-regulation of several key enzymes in the endogenous methylerythritol-5-phosphate (MEP)-dependent isoprenoid precursor pathway, as previously described (14). Accordingly, growth of the resulting recombinant *E. coli* cells in optimized minimal media enabled production of labeled miltiradiene from $^{13}C_6$-glucose. Using this methodology, fully ^{13}C-labeled miltiradiene was generated, as verified by GC–MS analysis (Fig. 2 *A* and *B*).

To reduce the amount of unlabeled tanshinones, *S. miltiorrhiza* hairy roots were subcultured, with addition of the general CPS inhibitor 2-Isopropyl-4-dimethylamino-5-methylphenyl-1-piperidinecarboxylate methyl Chloride AMO1618 (15), to suppress endogenous production of miltiradiene. Whereas it was possible to observe the incorporation of ^{13}C-labeled miltiradiene into the oxidized intermediate, ferruginol (Fig. 2 *C* and *D*), endogenous production levels were still sufficient to preclude detection of any other fully ^{13}C-labeled tanshinones (Fig. 1). This confounding endogenous metabolism was further suppressed by addition of the MEP pathway inhibitor, fosmidomycin (16, 17), as well as AMO1618, along with feeding increased amounts of labeled miltiradiene. Under these conditions, fully ^{13}C-labeled cryptotanshinone was observed (Fig. 2*E*), demonstrating that the labeled miltiradiene could undergo substantial elaboration and serve as a precursor to compounds found in the late stage of the proposed tanshinone biosynthetic pathway (Fig. 1).

CYP Candidate Gene Discovery. From our previous work with SmCPS and SmKSL, transcription of the encoding genes was clearly increased by induction of hairy root cultures (11). Such inducible transcription has been shown to extend to the subsequently acting CYPs in other terpenoid biosynthetic pathways (3, 18–24). Accordingly, to find candidate CYPs for tanshinone biosynthesis we moved beyond our previously reported EST database (9) and used next-generation sequencing of mRNA from induced hairy roots to generate an extensive transcriptome (accession no. SRX224100), resulting in 25,793 isotigs ranging from 100 to 1,100 nucleotides in length. Analysis of this dataset revealed the presence of ~300 CYP isotigs, close to the numbers of CYPs found in other plant species (22). Moreover, using an RNA-seq approach to examine the change in transcriptome upon induction with Ag^+, 14 CYP genes were selected as initial candidates for investigation on the basis of their significant increase in transcript levels.

Given the accumulation of tanshinones in the rhizome (8), and previous tissue-specific transcription demonstrated for other diterpenoid metabolism (18, 19, 25, 26), we hypothesized that tanshinone biosynthetic enzymes would be specifically expressed in the rhizome. Indeed, consistent with previous investigations (27), quantitative real-time (qRT)-PCR analysis demonstrated that SmCPS and SmKSL mRNA levels were higher in the rhizome than above ground tissues of *S. miltiorrhiza*. Hence, the relative expression of each of the 14 inducible CYPs was similarly analyzed, and transcripts for 6 of the 14 candidate CYPs were found to be more abundant in the rhizome. These 6 CYPs [GenBank accession nos. CYP76AH1 (JX422213), SmCYP-2 (JX422214), SmCYP-10 (JX422215), SmCYP-11 (JX422216), SmCYP-18 (JX422217), and SmCYP-20 (JX422218)] were then cloned to enable biochemical assays using miltiradiene as the substrate. As cytochrome P450 reductases (CPRs) are important to support the activities of CYPs, we also cloned full-length cDNA for two CPRs, SmCPR1 (GenBank accession no. CBX24555) and SmCPR2 (GenBank accession no. JX848592), that were present in our transcriptome. These two CPRs shared 79% nucleotide sequence

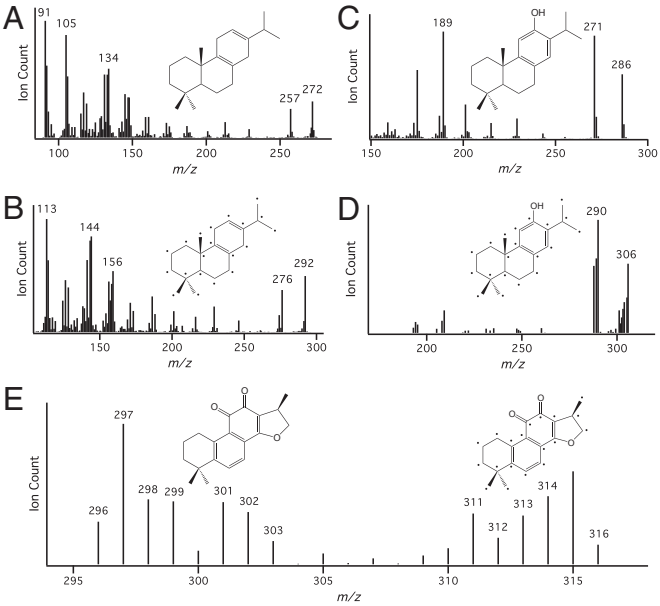

Fig. 2. Results of stable-isotope labeling experiments. Electrical ionization mass spectra of miltiradiene (*A* and *B*), ferruginol (*C* and *D*), and cryptotanshinone (*E*) from dashen hairy roots fed with unlabeled (*A* and *C*) or ^{13}C-labeled miltiradiene (*B*, *D*, and *E*).

identities (Fig. S1). Although SmCPR1 had been previously deposited, SmCPR2 seemed to be new.

CYP76AH1 Acts as a Ferruginol Synthase. The ability of these *S. miltiorrhiza* CYPs to react with miltiradiene was examined by recombinant expression in *S. cerevisiae*, followed by in vitro assays using microsomal preparations. Specifically, these six CYPs were expressed in the *S. cerevisiae* WAT11U strain, which expresses a CPR from *Arabidopsis thaliana* (AtCPR1), enabling more efficient reduction of plant CYPs (28). Microsomal preparations from the resulting recombinant yeasts were then assayed with miltiradiene, in the presence of NADPH, followed by GC–MS analysis. Notably, only one of these CYPs (designated CYP76AH1 by the Cytochrome P450 Nomenclature Committee; GenBank accession no. JX422213), was able to convert miltiradiene to an oxidized derivative (Fig. S2), which was determined to be ferruginol by comparison with an authentic standard (Fig. 3). None of the six CYPs was able to further react with ferruginol under identical assay conditions (Fig. S3). Steady-state kinetic analysis, in the presence of excess NADPH, indicated that CYP76AH1 efficiently catalyzes the conversion of miltiradiene into ferruginol, with k_{cat} = 4.4 ± 0.3 s^{-1} and K_M = 13 ± 3 μM (Fig. 4).

Coincidence of CYP76AH1 Transcription and Ferruginol Accumulation. To further strengthen the relevance of CYP76AH1 to ferruginol and tanshinone biosynthesis, we investigated ferruginol accumulation patterns. It has been reported that ferruginol accumulates along with tanshinones in *S. miltiorrhiza* suspension cells (29), as well as hairy roots (30). Tissue-specific analysis of whole plants demonstrated the expected accumulation of ferruginol in the rhizome, whereas none was detected in above-ground tissues, consistent with the *CYP76AH1* transcript accumulation pattern noted above. Moreover, we found that induction of hairy root cultures led to increased levels of ferruginol (Fig. 5*A*), tanshinones (Fig. S4), and *CYP76AH1* transcription (Fig. 5*B*), consistent with the hypothesized role for CYP76AH1 in ferruginol and, hence, tanshinone biosynthesis.

Assembling Pathways for Heterologous Ferruginol Production. In previous work, we assembled efficient pathways by using the modular pathway engineering (MOPE) approach and enabled the production of miltiradiene at levels of 365 mg/L in *S. cerevisiae* (12). This approach was applied here to realize heterologous production of ferruginol by additionally incorporating modules expressing *CYP76AH1* as well as a CPR gene. Initially, a CYP76AH1 (only) module, under the control of the transcription elongation factor 1 (TEF1) promoter, was added to the previously reported miltiradiene production vector, which contained the GGPP synthase (BTS1) and farnesyl diphosphate synthase (ERG20) fusion module BTS1-ERG20, the tHMG1 module for expressing the catalytic domain of hydroxy-3-methylglutaryl coenzyme A (tHMG1), and the copalyl diphosphate synthase (SmCPS) and kaurene synthase-like (SmKSL) fusion module SmKSL-SmCPS. The resulting plasmid was transformed into *S. cerevisiae* BY4741(ML) to give the engineered strain *S. cerevisiae* YJ32 (Fig. 6). However, whereas YJ32 produced considerable amounts of miltiradiene and geranylgeraniol (GGOH, produced by hydrolysis of GGPP), ferruginol was not detected (Fig. 6 and Fig. S5*A*). We hypothesized that the endogenous yeast CPR was incompetent to support the activity of the plant CYP76AH1. Accordingly, we turned to the use of the two *S. miltiorrhiza* CPRs, SmCPR1 and SmCPR2 to support the CYP76AH1 activity. The engineered strains YJ35 and YJ33, containing further assembled SmCPR1 module and SmCPR2 module on plasmid described above in the BY4741(ML), produced ferruginol at a titer of 10.5 and 5.2 mg/L, respectively, after 48 h of shake-flask fermentations. Interestingly, the production of miltiradiene and ferruginol by these strains was inversely correlated (Fig. S5). For example, YJ32 produced no ferruginol, but the highest miltiradiene titer of 5.2 mg/L, whereas YJ35 (contained SmCPR1) produced 10.5 mg/L of ferruginol and only 1.2 mg/L of miltiradiene. These observations indicated that the presence of a phyto-CPR was essential for CYP76AH1 to function in yeast. To further support this idea, the plasmids used for the construction of YJ32 and YJ35 were transformed into WAT11U (28), which harbors a chromosomally integrated copy of *AtCPR1* from *A. thaliana*, leading to engineered strains YJ42 and YJ45, respectively. As expected from our in vitro results described above, YJ42 produced ferruginol at 2.1 mg/L.

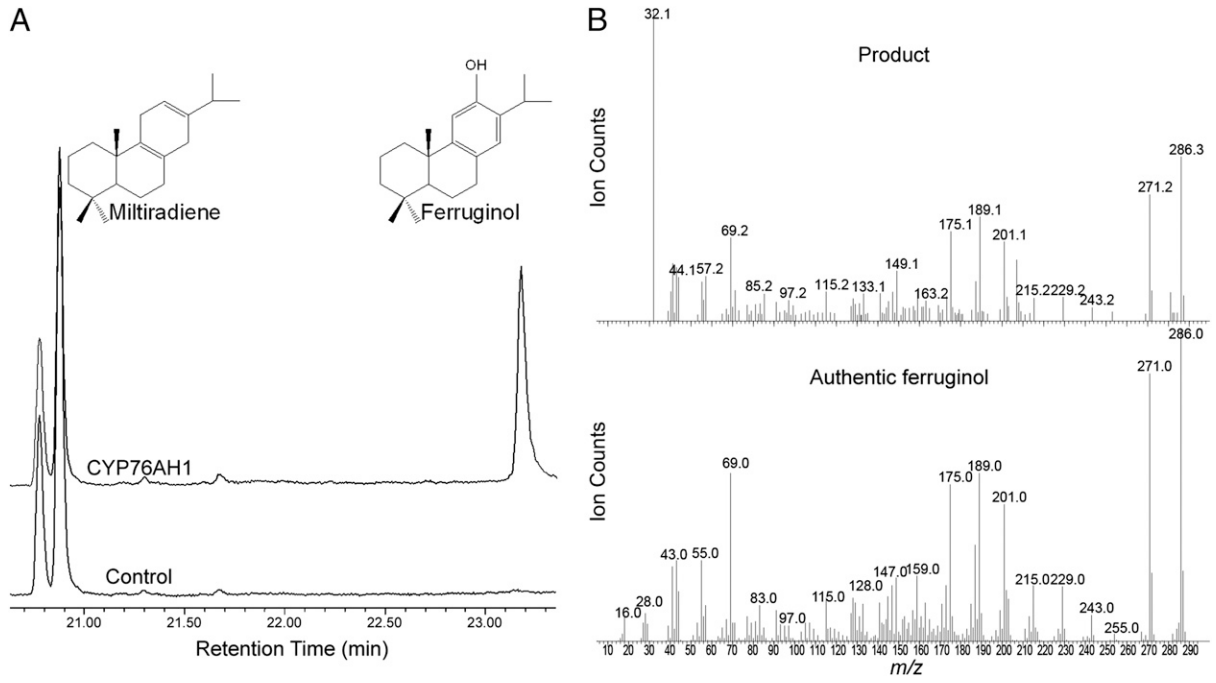

Fig. 3. Results of in vitro turnover of miltiradiene by CYP76AH1. (*A*) GC–MS chromatogram of extracts from the reaction containing CYP76AH1 microsomes with NADPH (*Upper* trace) and control (*Lower* trace). (*B*) Mass spectra of the reaction product compared with that of authentic ferruginol.

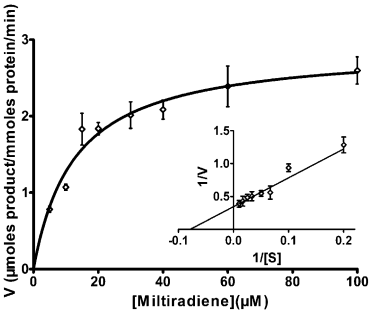

Fig. 4. Kinetic profile of CYP76AH1. Experimental details are included in *Materials and Methods*.

Interestingly, whereas YJ45 and YJ35 produced equal amounts of ferruginol, YJ45 accumulated significantly higher amounts of miltiradiene than YJ35 (Fig. S5 *C* vs. *D*). These results suggested that WAT11U provided greater metabolic flux to isoprenoid biosynthesis than BY4741(ML), although the copresence of AtCPR1 and SmCPR1 did not further improve ferruginol production levels. It should be mentioned that the specific ferruginol titers [milligrams per gram of dry cell weight (DCW)] followed similar trends to the volumetric titers (milligrams per liter) among all engineered strains (Fig. S6 vs. Fig. 6).

Discussion

We have previously reported functional identification of *S. miltiorrhiza* diterpene synthases, SmCPS and SmKSL, which catalyze the conversion of GGPP into the abietane-type diterpene olefin miltiradiene, a potential intermediate in the biosynthesis of the bioactive tanshinones of the important Chinese medicinal herb, danshen (11). Here we report stable-isotope labeling results that clearly demonstrate that miltiradiene is the precursor to at least two compounds found in the proposed tanshinone biosynthetic pathway, i.e., ferruginol and cryptotanshinone (Fig. 2). The implied formation of (crypto) tanshinones from miltiradiene requires extensive structural elaboration (Fig. S7). To understand the molecular bases of those transformations, we sought to identify the relevant genes, hypothesizing that the transcription of these would be inducible, as previously demonstrated for SmCPS and SmKSL (11). To provide a comprehensive foundation for these efforts, we undertook a next-generation sequencing-based functional genomics approach, to not only define the *S. miltiorrhiza* transcriptome, but also its transcriptional response to elicitor induction.

Miltiradiene is expected to undergo extensive oxidation, as well as carbon–carbon bond scission, to form diversified metabolites including tanshinones. Given that many of those biological transformations are typically carried out by CYPs (1), we focused on CYP-encoding genes whose transcription was coregulated with that of *SmCPS* and *SmKSL*, both in induction and rhizome tissue-specific expression patterns. From the six candidate CYPs identified through these criteria, we were able to demonstrate that one, CYP76AH1, readily converts miltiradiene into ferruginol in the presence of CPR1 from *A. thaliana* (Fig. 3). A number of other CYP76 family members have been shown to function in terpenoid biosynthesis (3, 24, 31). This notably includes four members of the CYP76M subfamily from rice that also function in diterpenoid metabolism (3, 24), two of which catalyze hydroxylation at C-11 of *ent*-cassadiene, a reaction that exhibits some similarity to the activity shown by CYP76AH1. Kinetic analysis of CYP76AH1 demonstrated not only high catalytic efficiency ($k_{cat}/K_M = 3.4 \times 10^5$ $M^{-1}{\cdot}s^{-1}$), but also a pseudosubstrate binding constant (K_M of 13 ± 3 μM) similar to that reported for the CYP76M subfamily members from rice diterpenoid biosynthesis, whose reported K_M values ranged from 2 to 40 μM (3, 24).

The ferruginol synthase activity exhibited by CYP76AH1 apparently requires a four-electron oxidation cascade. In particular, the production of ferruginol from miltiradiene involves both aromatization and the introduction of an oxygen atom at C-12 (Fig. S8). CYPs are known to catalyze dehydrogenation, as required for aromatization, as well as monooxygenation on a variety of carbon centers (32). Thus, the catalyzed reaction might follow an aromatization/monooxygenation sequence. Alternatively, the oxygen atom might be incorporated via epoxidation of the C-12,13 double bond, followed by ring opening and an additional oxidation step en route to ferruginol. Whereas detailed mechanistic insight awaits further biochemical characterization, CYP76AH1 nevertheless represents a unique enzyme that catalyzes a four-electron oxidation cascade on the cyclohexa-1,4-diene moiety to form a phenol moiety in tanshinone biosynthesis.

Ferruginol is a widespread diterpenoid metabolite, and has been found in the Podocarpaceae (33), the Cupressaceae (34), the Lamiaceae (35), and the Verbenaceae (36) plant families. Notably, a transcriptome recently has become available for the perennial herb rosemary (*Rosmarinus officinalis*; http://medicinalplantgenomics.msu.edu), which also is known to produce ferruginol, and this contains several isotigs that exhibit close homology to CYP76AH1 (~85% nucleotide sequence identity; Fig. S9). Isotig homologs to SmCPS and SmKSL also can be found in the rosemary transcriptome, indicating that our results from investigating tanshinone biosynthesis will be more widely applicable to the metabolism of other plant diterpenoid natural products. Indeed, ferruginol serves as a potential intermediate for the carnosic acid produced by rosemary. In turn, carnosic acid also may be an intermediate in tanshinone biosynthesis (Fig. 1 and Fig. S7). Intriguingly, phylogenetic analysis revealed that four of the remaining five danshen CYPs whose expression pattern matches that of tanshinone accumulation are closely related to CYP99A3 (Fig. S9), which catalyzes the conversion of the C-19 methyl of diterpene momilactone to a carboxylic acid in rice (21). Particularly given the similar transformations required for tanshinone biosynthesis (e.g., oxidative loss of C-19 and C-20 in formation of tanshinone I), these CYPs seem likely to be involved in downstream transformations for tanshinone biosynthesis. We thus prepared microsome samples from recombinant yeasts harboring these CYP genes and performed reactions using ferruginol as the substrate; however, no product was observed (Fig. S3).

Ferruginol further serves as a bioactive natural product in its own right, and has been shown to exhibit a range of activities similar to that of the tanshinones (37). Given that it also can be found in *S. miltiorrhiza* rhizomes, ferruginol may contribute to the medicinal effect of danshen. In part based on the potential use of ferruginol itself, we assembled synthetic pathways for microbial production of ferruginol in yeast. Whereas incorporating CYP76AH1 alone into the miltiradiene-producing yeast strain failed to produce ferruginol, yeast strains harboring CYP76AH1 in the presence of plant CPRs from *S. miltiorrhiza* or *A. thaliana* produced ferruginol (Fig. 6). Under flask-shake conditions without process optimization, we achieved a ferruginol titer of 10.5 mg/L, which was comparable to the result obtained in

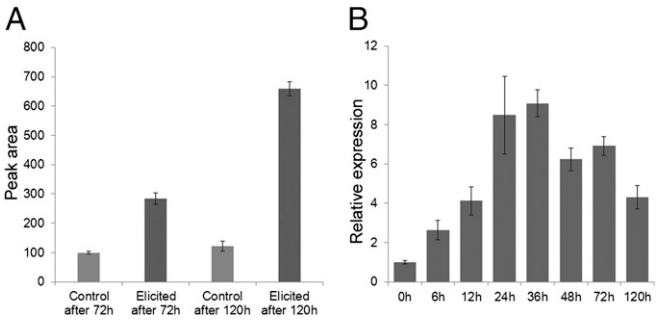

Fig. 5. Correlation of gene expression of *CYP76AH1* and ferruginol accumulation. (*A*) Accumulation of ferruginol in hairy roots responding to Ag^+ induction. (*B*) Real-time PCR analysis of *CYP76AH1* mRNA level in hairy roots of danshen after exposure to Ag^+.

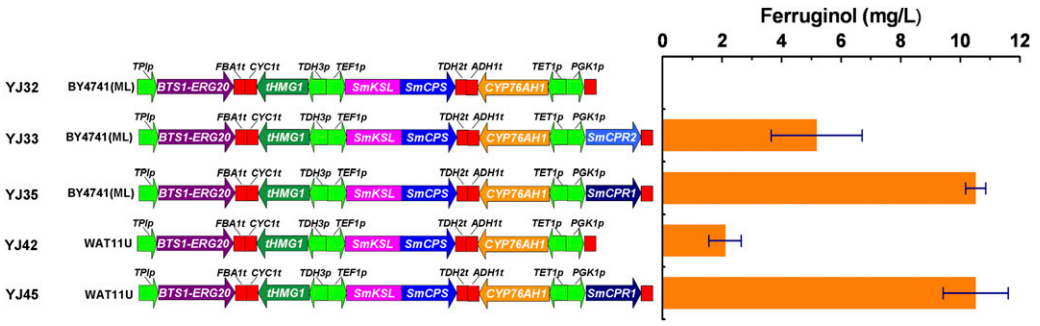

Fig. 6. Results of the assembled ferruginol production pathways. Yeast strains were cultivated in a ZWY-1102 shaking incubator (Shanghai Zhicheng) with 100 mL YPD media at 30 °C, 200 rpm for 48 h. All data represent the averages ± SDs of three independent clones.

E. coli for the production of the first CYP modified taxadiene, taxadien-5α-ol, a precursor to taxol (38). Furthermore, we expected that it should be possible to significantly increase ferruginol yield via a combination of strain engineering and process optimization (12, 39).

In conclusion, here we have established the intermediacy of miltiradiene in the biosynthesis of the bioactive tanshinone diterpenoids from the Chinese medicinal herb *S. miltiorrhiza* (danshen), and used a next-generation sequencing-based approach to functionally identify the relevant ferruginol synthase, CYP76AH1. The results and approaches described here provide a solid foundation for further investigation of not only the biosynthesis of the tanshinones, but that of plant labdane-related diterpenoids more generally. As there is strong interest in microbial production of phytoditerpenoids (12, 14, 38, 39), our metabolic engineering efforts reported here also will facilitate the construction of such microbial cell factories.

Materials and Methods

Isolation and Quantification of Ferruginol. Analysis of ferruginol levels was carried out much as previously described (29). Briefly, dried and powered hairy roots were extracted with ethyl acetate, with fivefold concentration of these extracts used for ferruginol quantification by GC analysis. GC analyses were carried out using an Agilent GC7890 system with HP-5 column (320 μm × 0.25 μm × 30 m) and flame ionization detection, with quantification by comparison with an authentic standard for ferruginol, which was obtained from WUXI APPTEC Co.. Samples (1 μL) were injected in splitless mode at 280 °C. The GC oven temperature was programmed to increase at 6 °C/min from 150 °C to 220 °C, at 3 °C/min from 220 °C to 230 °C, and at 20 °C/min from 230 °C to 280 °C.

Isolation of Total RNA and qRT-PCR Analysis. For *CYP76AH1* expression analysis, hairy roots were induced with Ag^+, and sampled after 6 h, 12 h, 24 h, 48 h, 72 h, and 120 h. Total RNA was extracted from hairy roots using TRIzol reagent (Invitrogen) following the manufactures' directions. First-strand cDNA was synthesized with RevertAid First Strand cDNA synthesis Kit (Fermentas) using oligo $(dT)_{18}$ primer. Quantitative real-time PCR was performed using the SYBR Premix Ex Taq (Takara Bio) and an Applied Biosynthesis 7500 Real-Time machine. The primers used were: 5′-TCGTGGATGAGTCGGCAAT-3′ and 5′-TGAGTATCTGAGTTCCCT-3′. Actin was used as the endogenous control to normalize expression value. At least three independent experiments were performed for each analysis (tissues and time points).

cDNA Cloning and Heterologous Expression of CYP76AH1 in Yeast. The 5′ and 3′ ends of the targeted CYP and SmCPR2 were cloned by RACE (Invitrogen) according to the manufacturer's directions. Full-length cDNA was cloned from cDNA isolated from induced hairy roots 12 h after induction with Ag^+, using PrimeStar DNA polymerase (Takara Bio). The ORF region of *CYP76AH1* was subcloned into yeast epitope-tagging vector pESC-His via *EcoR* I and *Spe* I digestion with PCR amplification using primers shown in Table S1. The pESC-His-CYP76AH1 construct was verified by complete gene sequencing, which was transformed into the yeast strain WAT11U (28). Transformants were selected on synthetic dropin medium −His (SD−his) containing 20 g/L glucose and grown at 28 °C for 48 h. The resulting recombinant strain was initially grown in SD−His liquid medium with 20 g/L glucose at 28 °C for about 48 h to an OD_{600} of 2–3. Cells were centrifuged and washed three times with sterile water to remove any residual glucose. The cells were then resuspended in the yeast peptone galactose (YPL) induction medium (10 g/L yeast extract, 20 g/L bactopeptone, and 20 g/L galactose) and grown overnight at 28 °C to induce recombinant protein expression. ORFs of *SmCYP-2, SmCYP-10, SmCYP-11, SmCYP-18,* and *SmCYP-20* were also subcloned into pESC-His as done for *CYP76AH1*, and transformants were generated and confirmed by sequencing.

In Vitro Enzymatic Activity Assay. Miltiradiene samples were prepared using our engineered yeasts as described (30). Microsomes were prepared as previously described (40). Microsomal membranes were suspended in storage buffer containing 50 mM Tris·HCl (pH 7.5), 1 mM EDTA, and 20% (vol/vol) glycerol. Initial in vitro hydroxylation assays were conducted in a total volume of 500 μL of 90 mM Tris·HCl (pH 7.5), containing 1 mM NADPH, 500 μg of microsomal protein, and 100 μM miltiradiene. The assays were incubated with shaking for 3 h at 28 °C, and the reactions terminated by extraction with an equal volume of ethyl acetate. These extracts were directly analyzed by GC–MS using an Agilent 6890 GC–MS system with an HP-5MS capillary column (250 μm × 0.25 μm × 30 m; J & W Scientific). Analysis was carried out on 4-μL samples with splitless injection at 225 °C. The GC oven temperature was programmed to increase at 10 °C/min from 70 °C to 280 °C.

Kinetic Analysis. For kinetic analysis, CYP76AH1 concentration was estimated by measuring the reduced CO-binding difference spectra using an extinction coefficient of 91 $mM^{-1}{\cdot}cm^{-1}$ as reported (41). Experiments were carried out using serial concentrations of miltiradiene: 5 μM, 10 μM, 15 μM, 20 μM, 30 μM, 40 μM, 60 μM, and 100 μM, in 1-mL enzyme assays. These also contained 1 mg microsomal protein (0.011 μmol CYP76AH1) in 90 mM Tris·HCl (pH 7.5), with 0.5 mM NADPH along with a regenerating system (consisting of 5 μM FAD, 5 μM FMN, 5 mM glucose-6-phosphate, 0.5 unit/mL glucose-6-phosphate dehydrogenase, and 2 mM DTT). Reactions were initiated by substrate addition, incubated with shaking at 28 °C for 30 min, and then terminated by extracting three times with 1 mL of ethyl acetate, with 0.5 μM octadecane as an internal standard. Pooled extracts were completely evaporated under N_2 and then dissolved in 50 μL ethyl acetate for quantification by GC analysis, carried out as described above. K_M and k_{cat} values were calculated by nonlinear regression using GraphPad Prism version 5.04, and the data reported are the means ±SD from triplicate analyses.

Engineering Yeasts for Ferruginol Production. The yeast strain BY4741(ML) was constructed by complementing the auxotrophic markers LEU2 (encoding β-isopropylmalate dehydrogenase) and MET15 (encoding O-acetylhomoserine/O-acetylserine sulfhydrylase) in the BY4741 strain as previously described (12). Synthetic pathways were assembled according to the MOPE strategy, consisted of the previously described BTS1-ERG20 module, overexpressing the fusion protein of GGPP synthase and farnesyl diphosphate synthase, tHMG1 module, overexpressing a truncated hydroxy-3-methylglutaryl reductase, SmKSL-SmCPS module, overexpressing the fused diterpene synthase (12), along with the CYP76AH1 module, and the SmCPR1 module or the SmCPR2 module described here. The primers used in this work are listed in Table S1. These constructs were transformed into the yeast strains BY4741(ML) or WAT11U, resulting in strains engineered for ferruginol production (Table S2). Cells were grown in SC medium lacking uracil at 30 °C, shaking at 200 rpm for 48 h in a ZWY-1102 shaking incubator (Shanghai Zhicheng), and then transferred to 100 mL of YPD medium in 500-mL flasks to an initial OD_{600} of 0.05, and cultivated for another 48 h. Terpenoid products were extracted as previously described (12) and analyzed by GC using a 7890F system (Techcomp Scientific Instrument Co.) with flame ionization detector, and equipped with an SE-54 column (250 μm × 0.25 μm × 30 m). Column pressure was kept at 0.10 MPa, with 4.5 mL/min carrier gas (N_2) flow rate. The injector and detector

temperatures were 270 °C and 290 °C, respectively, with oven temperature maximum of 250 °C.

Plant Materials, Miltiradiene Labeling, and Feeding Studies. Details of plant materials preparation and analysis; miltiradiene labeling; and the feeding of labeled miltiradiene to freshly subcultured hairy root cultured are given in *SI Materials and Methods*.

ACKNOWLEDGMENTS. We thank Prof. Oliver Yu for the gift of yeast expression strain WAT11U and the expression vector, as well as expression advice; Prof. Ming Yan for providing vector pYX212; and Prof. Lingjian Wang, Prof. Wenli Hu, and Ms. Xiaohui Ma for their kind assistance. This work was supported by National Natural Science Foundation of China Grants 81072990 and 81202871 (to L.H.), National Basic Research and Development Program of China Grant 2012CB721103 (to Z.K.Z.), and National Institutes of Health Grant GM086281 (to R.J.P.).

1. Mizutani M (2012) Impacts of diversification of cytochrome P450 on plant metabolism. *Biol Pharm Bull* 35(6):824–832.
2. Mizutani M, Ohta D (2010) Diversification of P450 genes during land plant evolution. *Annu Rev Plant Biol* 61:291–315.
3. Wang Q, et al. (2012) Characterization of CYP76M5-8 indicates metabolic plasticity within a plant biosynthetic gene cluster. *J Biol Chem* 287(9):6159–6168.
4. Jiang M, Stephanopoulos G, Pfeifer BA (2012) Downstream reactions and engineering in the microbially reconstituted pathway for Taxol. *Appl Microbiol Biotechnol* 94(4): 841–849.
5. Wang X, Morris-Natschke SL, Lee K-H (2007) New developments in the chemistry and biology of the bioactive constituents of Tanshen. *Med Res Rev* 27(1):133–148.
6. Tian P (2011) Convergence: Where West meets East. *Nature* 480(7378):S84–S86.
7. Xu Z (2011) Modernization: One step at a time. *Nature* 480(7378):S90–S92.
8. Wang JW, Wu JY (2010) Tanshinone biosynthesis in *Salvia miltiorrhiza* and production in plant tissue cultures. *Appl Microbiol Biotechnol* 88(2):437–449.
9. Cui G, Huang L, Tang X, Zhao J (2011) Candidate genes involved in tanshinone biosynthesis in hairy roots of *Salvia miltiorrhiza* revealed by cDNA microarray. *Mol Biol Rep* 38(4):2471–2478.
10. Peters RJ (2010) Two rings in them all: The labdane-related diterpenoids. *Nat Prod Rep* 27(11):1521–1530.
11. Gao W, et al. (2009) A functional genomics approach to tanshinone biosynthesis provides stereochemical insights. *Org Lett* 11(22):5170–5173.
12. Zhou YJ, et al. (2012) Modular pathway engineering of diterpenoid synthases and the mevalonic acid pathway for miltiradiene production. *J Am Chem Soc* 134(6): 3234–3241.
13. Cyr A, Wilderman PR, Determan M, Peters RJ (2007) A modular approach for facile biosynthesis of labdane-related diterpenes. *J Am Chem Soc* 129(21):6684–6685.
14. Morrone D, et al. (2010) Increasing diterpene yield with a modular metabolic engineering system in *E. coli*: Comparison of MEV and MEP isoprenoid precursor pathway engineering. *Appl Microbiol Biotechnol* 85(6):1893–1906.
15. Dennis DT, Upper CD, West CA (1965) An enzymic site of inhibition of gibberellin biosynthesis by Amo 1618 and other plant growth retardants. *Plant Physiol* 40(5): 948–952.
16. Kuzuyama T, Shizimu T, Takahashi S, Seto H (1998) Fosmidomycin, a specific inhibitor of 1-deoxy-d-xylulose 5-phosphate reductoisomerase in the nonmevalonate pathway of isoprenoid biosynthesis. *Tetrahedron Lett* 39:7913–7916.
17. Zeidler J, et al. (1998) Inhibition of the non-mevalonate 1-deoxy-d-xylulose-5-phosphate pathway of plant isoprenoid biosynthesis by fosmidomycin. *Z Naturforsch C* 53:980–986.
18. Hamberger B, Ohnishi T, Hamberger B, Séguin A, Bohlmann J (2011) Evolution of diterpene metabolism: Sitka spruce CYP720B4 catalyzes multiple oxidations in resin acid biosynthesis of conifer defense against insects. *Plant Physiol* 157(4):1677–1695.
19. Ro DK, Arimura G, Lau SY, Piers E, Bohlmann J (2005) Loblolly pine abietadienol/abietadienal oxidase PtAO (CYP720B1) is a multifunctional, multisubstrate cytochrome P450 monooxygenase. *Proc Natl Acad Sci USA* 102(22):8060–8065.
20. Shimura K, et al. (2007) Identification of a biosynthetic gene cluster in rice for momilactones. *J Biol Chem* 282(47):34013–34018.
21. Wang Q, Hillwig ML, Peters RJ (2011) CYP99A3: Functional identification of a diterpene oxidase from the momilactone biosynthetic gene cluster in rice. *Plant J* 65(1): 87–95.
22. Nelson DR, Schuler MA, Paquette SM, Werck-Reichhart D, Bak S (2004) Comparative genomics of rice and Arabidopsis. Analysis of 727 cytochrome P450 genes and pseudogenes from a monocot and a dicot. *Plant Physiol* 135(2):756–772.
23. Wu Y, Hillwig ML, Wang Q, Peters RJ (2011) Parsing a multifunctional biosynthetic gene cluster from rice: Biochemical characterization of CYP71Z6 & 7. *FEBS Lett* 585(21):3446–3451.
24. Swaminathan S, Morrone D, Wang Q, Fulton DB, Peters RJ (2009) CYP76M7 is an entcassadiene C11α-hydroxylase defining a second multifunctional diterpenoid biosynthetic gene cluster in rice. *Plant Cell* 21(10):3315–3325.
25. Wilderman PR, Xu M, Jin Y, Coates RM, Peters RJ (2004) Identification of *syn*-pimara-7,15-diene synthase reveals functional clustering of terpene synthases involved in rice phytoalexin/allelochemical biosynthesis. *Plant Physiol* 135(4):2098–2105.
26. Xu M, Hillwig ML, Prisic S, Coates RM, Peters RJ (2004) Functional identification of rice *syn*-copalyl diphosphate synthase and its role in initiating biosynthesis of diterpenoid phytoalexin/allelopathic natural products. *Plant J* 39(3):309–318.
27. Ma Y, et al. (2012) Genome-wide identification and characterization of novel genes involved in terpenoid biosynthesis in *Salvia miltiorrhiza*. *J Exp Bot* 63(7):2809–2823.
28. Urban P, Mignotte C, Kazmaier M, Delorme F, Pompon D (1997) Cloning, yeast expression, and characterization of the coupling of two distantly related *Arabidopsis thaliana* NADPH-cytochrome P450 reductases with P450 CYP73A5. *J Biol Chem* 272(31):19176–19186.
29. Miyasaka H, Nasu M, Yamamoto T, Endo Y, Yoneda K (1986) Regulation of ferruginol and cryptotanshinone biosynthesis in cell suspension cultures of *Salvia miltiorrhiza*. *Phytochemistry* 25:637–640.
30. Zhi BH, Alfermann AW (1993) Diterpenoid production in hairy root cultures of *Salvia miltiorrhiza*. *Phytochemistry* 32:699–703.
31. Collu G, et al. (2001) Geraniol 10-hydroxylase, a cytochrome P450 enzyme involved in terpenoid indole alkaloid biosynthesis. *FEBS Lett* 508(2):215–220.
32. Sono M, Roach MP, Coulter ED, Dawson JH (1996) Heme-containing oxygenases. *Chem Rev* 96(7):2841–2888.
33. Bispo de Jesus M, et al. (2008) Ferruginol suppresses survival signaling pathways in androgen-independent human prostate cancer cells. *Biochimie* 90(6):843–854.
34. Sharp H, et al. (2001) Totarol, totaradiol and ferruginol: Three diterpenes from *Thuja plicata* (Cupressaceae). *Biochem Syst Ecol* 29(2):215–217.
35. Yang MH, Blunden G, Xu YX, Nagy G, Máthé I (1996) Diterpenoids from *Salvia* species. *Pharm Pharmacol Commun* 2:69–71.
36. Ono M, et al. (1999) Diterpenes from the fruits of *Vitex rotundifolia*. *J Nat Prod* 62(11):1532–1537.
37. Tada M, et al. (2000) Synthesis of (+)- and (–)-ferruginol via asymmetric cyclization of a polyene. *J Chem Soc, Perkin Trans 1* (16):2657–2664.
38. Ajikumar PK, et al. (2010) Isoprenoid pathway optimization for Taxol precursor overproduction in *Escherichia coli*. *Science* 330(6000):70–74.
39. Kirby J, Keasling JD (2009) Biosynthesis of plant isoprenoids: Perspectives for microbial engineering. *Annu Rev Plant Biol* 60:335–355.
40. Pompon D, Louerat B, Bronine A, Urban P (1996) Yeast expression of animal and plant P450s in optimized redox environments. *Methods Enzymol* 272:51–64.
41. Omura T, Sato R (1964) The carbon monoxide-binding pigment of liver microsomes II solubilization, purification and properties. *J Biol Chem* 239:2379–2385.